ELSEVIER

Nuclear Instruments and Methods in Physics Research A 447 (2000) 61–68

NUCLEAR INSTRUMENTS & METHODS IN PHYSICS RESEARCH Section A

www.elsevier.nl/locate/nima

Status of the HERA-B vertex detector

C. Bauer[a], M. Bräuer[a], T. Glebe[a], W. Hofmann[a], T. Jagla[a], K.T. Knöpfle[a], V. Pugatch[1a], M. Schmelling[a], B. Schwingenheuer[a,*], E. Sexauer[a], L. Seybold[a], U. Trunk[a], R. Wanke[a], I. Abt[b], M. Dressel[b], S. Masciocchi[b], B. Moshous[b], T. Perschke[b], K. Riechmann[b], M. Sang[b], S. Schaller[b], W. Wagner[b], M. Merk[c], M. Mevius[c], A. van den Brink[c]

[a]*Max-Planck-Institut für Kernphysik, Postfach 10 39 80, D-69029 Heidelberg, Germany*
[b]*Max-Planck-Institut für Physik, Föhringer Ring 8, D-80804 München, Germany*
[c]*Universiteit Utrecht, Vakgroep Subatomaire Fysica, Princetonlaan 4, NL-3584 CB Utrecht, The Netherlands*

Abstract

The HERA-B experiment is a forward magnetic spectrometer with good particle identification for hadrons and leptons designed to study violation of CP symmetry in the neutral B meson system. The silicon vertex detector operates in a high-rate environment similar to the ones expected at LHC. In this paper we report on our R&D on strip detector design, frontend ASICs, mechanical and thermal engineering, low-mass RF shielding of the HERA proton beam and on the status of our reconstruction software. First experiences with last year's installation are discussed.

1. Introduction

HERA-B is a fixed target experiment [1] at the HERA storage ring at DESY, Hamburg. In the experiment 920 GeV/c protons interact with up to eight wires positioned in the radial tail of the beam and produce $b\bar{b}$ quarks at a rate of about 10^{-6}/interaction. These quarks fragment independently into B hadrons and their decay products and vertices are reconstructed with the HERA-B apparatus. Of special interest is the decay $B^0, \bar{B}^0 \to J/\Psi K_S$ since a large CP violating rate difference is expected between B^0 and $\bar{B}^0$. To observe a sizeable number of events the wires are positioned such that there are on average four interactions every 96 ns bunch crossing. This collision rate of 40 MHz poses severe requirements on radiation hardness, detector granularity, DAQ bandwidth and trigger performance.

The reconstruction of B meson decay vertices displaced from the primary vertex at the Level 2 trigger stage is already mandatory to suppress background. The technology of choice for the vertex Detector (VDS) is double-sided silicon strip detectors. Table 1[2] contains a list of design

* Corresponding author.
E-mail address: b.schwingenheuer@mpi-hd.mpg.de (B. Schwingenheuer).

[1] Permanent address: Institute for Nuclear Research, Ukrainian Academy of Science, 252028 Kiev, Ukraine.

[2] HalbLeiterLabor, the Semiconductor Laboratory of the Max-Planck-Institutes in Munich, Germany.

0168-9002/00/$ - see front matter
PII: S0168-9002(00)00173-X

Table 1
Parameters of the double-sided silicon strip detectors

Dimension	53 mm × 73 mm, 280 μm thick
Active area	50 mm × 70 mm
Structure	n bulk with "p on n" and "n on n" strips
Isolation	p-stop (Sintef detectors) or p-spray (HLL detectors)
Readout pitch	51.7 μm on n-side, 54.6 μm on p-side, (1280 × 1024 strips)
Implant width	15 μm
Intermediate strips	Yes (except for n-side of Sintef detectors)
Strip angle	2.5° w.r.t. wafer edge
Bias resistor	Polysilicon, resistivity ≈ 1 MΩ
V_{FD}	40 V, 100 V or 130 V depending on production batch
Coupling	AC coupling (to HELIX128-2.2 chip)

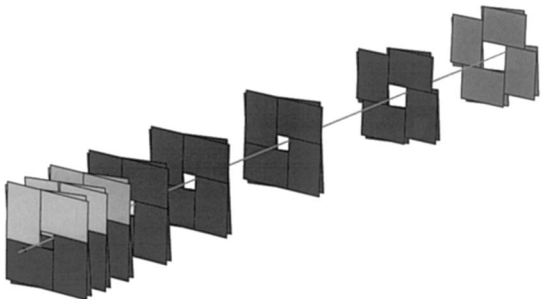

Fig. 1. Isometric view of the VDS. The current installation includes all dark-shaded strip detectors. The distances from the target vary from 5 cm to 2 m. In reality the wafers are not rotated by 2.5° (as drawn) but the strips w.r.t. the wafer edge.

parameters of the detectors [2,3] and Fig. 1 shows the geometrical arrangement of the VDS. Sixty-four strip detectors are positioned in eight superlayers such that every track originating from the target at an angle between 10 and 250 mrad passes through at least three layers. The dark-shaded detectors are currently installed and the rest will be installed by the end of the year. Four track projections per superlayer are measured: $\pm 2.5°, 87.5°$ and 92.5°. Thus, trajectories are measured with some redundancy and standalone track reconstruction is feasible.

Radially, the silicon detectors are separated from the beam by 10 mm. For the innermost active area the fluence is expected to be similar to LHC experiments [4]. To reduce leakage current noise it is foreseen to cool the strip detectors and to exchange the damaged modules annually. Irradiation tests of a strip detector have been performed to estimate the performance after one year (Section 2).

For readout the HELIX chip was developed in collaboration with the University of Heidelberg (Section 3).

During proton injection a larger aperture of 20 mm is needed. This has considerable impact on the mechanical design of the VDS: for all but the last superlayer the strip detectors are mounted in Roman Pots, i.e. every quadrant of a superlayer is equipped with a manipulator for lateral and radial movements. The mechanical assembly inside a Roman Pot is described in Section 4.

The target and the first seven superlayers are housed in a 2.5 m long vacuum tank whose shape is determined by the 250 mrad acceptance angle. This vessel is part of the storage ring and special precaution is taken to reduce wake fields in the tank (Section 4).

Section 5 discusses the readout chain and Section 6 the experience gained so far from last year's installation at DESY.

2. Irradiation test of a strip detector

In HERA-B the silicon detectors will experience a strongly non-uniform irradiation profile (even along the strips) since the flux is expected to fall with $1/r^2$ with r being the distance from the proton beam. Furthermore the maximal fluence accumulated over one year is large, about 3×10^{14} MIPS/cm^2. A priori it is not clear that the performance of the detector is acceptable after one HERA-B year and previous irradiation tests with strip detectors using punch-through biasing [5–7] showed an intolerable noise increase, presumably due to $1/f$ noise [8]. Here we present results from irradiation tests of a single-sided strip detector (p strips on n-type bulk).

We used 195 MeV/c protons delivered by the Tandem accelerator at the MPI Heidelberg and scattered them off a 50 μm thick gold foil. Protons hitting the detector have scattered between 7° and 23°. Fig. 2 shows the average fluence versus the

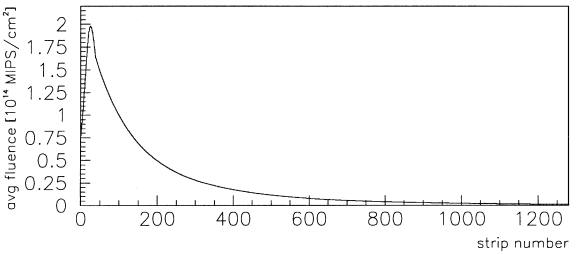

Fig. 2. MIPS equivalent average fluence versus strip number for the irradiated detector. The strip length and thus the fluence grows linearly for the first 40 strips because of the stereo angle.

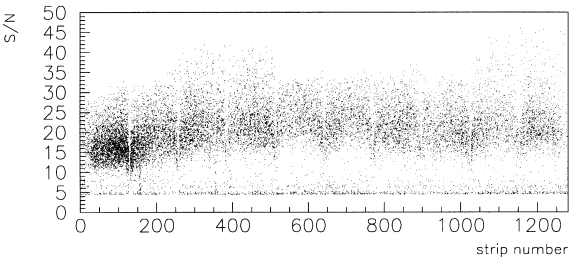

Fig. 3. Cluster charge over strip noise (S/N) versus strip number.

strip number of the detector. A scale factor of 3 is applied to scale from the damage of protons to the one from MIPS [9].

Because of the 2.5° stereo angle, the length of the first 40 strips rises linearly and the same applies to the fluence. The peak fluence of 3×10^{14} MIPS/cm^2 results in a full-depletion voltage of 450 V (two months after the exposure and storage at 10°C). The leakage current is about 800 μA at 10°C. Strips with numbers larger than 1000 experienced almost no damage.

The most relevant question of the irradiation test concerns the cluster signal over the strip noise (S/N) performance. This was measured with a ^{106}Ru β-source. After passing through the strip detector the electrons were stopped in a scintillator whose discriminated signal was used as a trigger. The threshold corresponded to a minimum electron momentum of about 2 MeV/c, ensuring that the energy deposited in the silicon is close to that of a MIP.

The entire readout chain was identical to the one used at HERA-B. Fig. 3 shows the S/N versus strip number. The strip detector is fully functional in all regions (type-inverted for strip numbers <550, compensated from strip numbers 550–950 and original n-type material for strip numbers >950). Clearly visible is the separation between the tail of noise clusters (small S/N) and the electron hits (S/N of 14 for the most irradiated strips and 21 for the undamaged strips). Note that the cluster shape does not depend on the irradiation level, i.e. the average width is about 2.8 strips in all regions of the detector, and the charge sharing between neighboring strips is unaffected by irradiation.

Obviously, this result is very encouraging since detector operation seems possible after one year and the noise increase is tolerable. More details of this study can be found in Ref. [10].

3. Readout chip

The main specifications for the readout chip are a latency of 12 μs, a shaping time equivalent to the bunch spacing of 96 ns, moderate radiation hardness[3] (about 1 kGy) and a deadtimeless readout within 20 μs, i.e. internal buffers for multiple triggers. The noise at an input load of 20 pF should be small enough to result in a S/N of about 20 for a signal of 24 000e$^-$.

At the time of the Technical Design Report [1] no chip was available with these specifications, although chip developments for LHC were under way. It was therefore decided to design a chip ourselves in collaboration with the University of Heidelberg [11]. This effort was based on the architecture of the FELIX chip [12] and turned out to be very successful. The Version 2.2 of the so-called HELIX chip [13–15] fulfills all requirements.[4]

The chip is still operational after a dose of 4 kGy and the degradation in noise performance is tolerable at the expected level of 1 kGy (Fig. 4). More details can be found in Ref. [14].

[3] To reduce irradiation dose and material within the acceptance the readout chips are positioned at 100 mm from the beam.

[4] A few remaining problems do not compromise the operation.

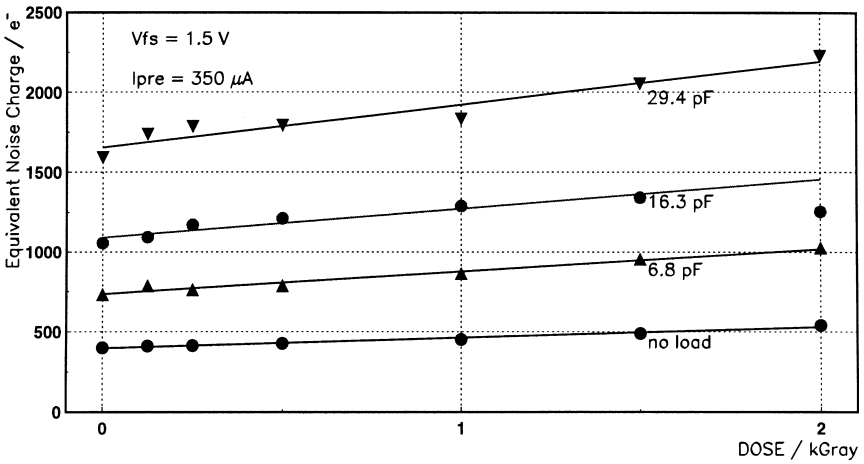

Fig. 4. Noise of the HELIX128-2.2 versus dose for different input loads.

4. Mechanical module assembly

Fig. 5 shows the mechanical assembly of two double-sided strip detectors which form a quadrant of one superlayer, called module. Tests have shown that the glue for attaching the wafer to the mechanical support is critical for double-sided detectors. A silicone-based adhesive which remains elastic avoids mechanical stress on the detector surface [16].

The mechanical supports are constructed from a carbon fiber matrix based on the K1100X fiber[5] with $\lambda X_0 = 110$ W/K, or a carbon fiber–graphite matrix (TPG)[6] with $\lambda X_0 = 270$ W/K. The dimensions of the plates should be chosen such that the silicon temperature can be maintained at 0°C when the cooling block, which is outside of the acceptance, is at -15°C. Note that the plates have a fork-like layout at the position of the silicon to reduce material in the active area. Averaged over the active area one module amounts to 1.2% X_0.

While the detector is separated by 10 mm from the beam this distance is 100 mm for the hybrids with the HELIX chips. Every hybrid (270 μm thick Al_2O_3) contains reference resistors, blocking capacitors and 10 or 8 chips for the n-side or p-side readout, respectively. It has its own carbon fiber carrier to separate the cooling path of the HELIXes from the one for the detector. Aluminium foils between the carriers reduce heating of the detector by thermal radiation from the hybrid carriers.

The connection between the strip detector and the chips is done with flex-jumpers:[7] 4-layer Kapton cables with 8 μm thick copper traces adapting the detector pitch to the chip pitch (41.4 μm).

The cooling block is outside of the acceptance. A channel is milled into the copper block and a cooling pipe, which is bent to fit into the channel, is brazed to the block. This way the cooling pipe is seamless inside the vacuum (no weld) and the chance of a water leak is minimized. Binary ice[8] at a temperature of -4°C and below is used as coolant. The heat conduction between the carbon fibers and the cooling block is improved with silver epoxy.

[5] Produced by Amaco, USA. The heat conduction coefficient λ was measured to be 470 ± 40 W/mK for our matrix layout and X_0 was scaled from carbon according to the measured density of the matrix.

[6] Produced by Advanced Ceramics, USA. λ was measured to be 1270 ± 60 W/mK for our layout and X_0 was scaled from carbon.

[7] Produced by Dyconex, Switzerland.

[8] Produced by Integral Energietechnik, Germany.

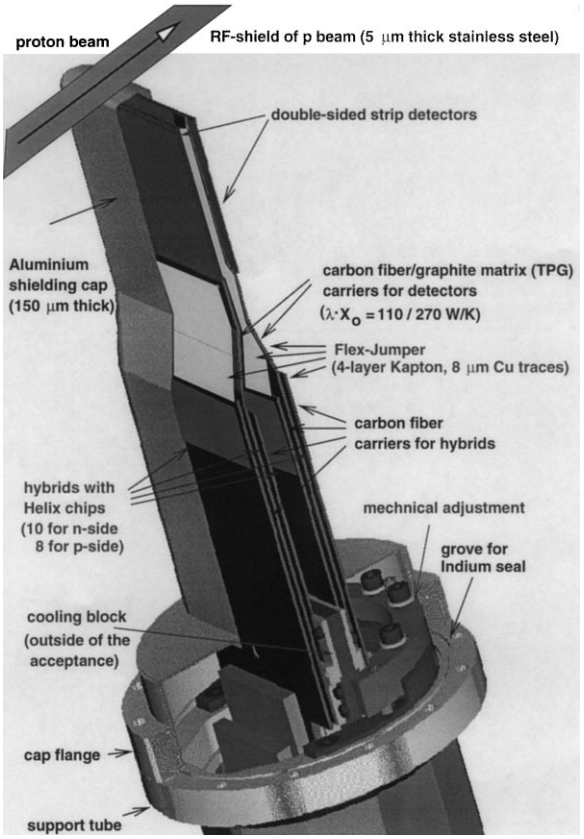

Fig. 5. Detector module with two double-sided strip detectors. Depending on the distance of the superlayer from the target the length of the detector carrier varies from 150 to 430 mm.

The modules are operated in a secondary vacuum. Protection against RF pick-up from the beam and separation from the primary vacuum of the ring is provided by 150 μm thick aluminium caps. A cap is produced as a single piece by galvanic deposition of aluminium on a stainless steel nucleus.[9] In this process it is possible to avoid adherence of the two metals. After the final growth thickness is reached the aluminium can be removed from the nucleus at high temperatures. The thin cap is electron-beam welded to the flange[10] and mounted to the stainless-steel support tube, i.e. the Roman Pot. An indium wire seals the secondary from the primary vacuum.

Vacuum feedthroughs (atmosphere to secondary vacuum) for cooling and electrical signals are located at the other end of the support tube and pipes and cables are routed inside the tube. Everything is assembled in the laboratory and then the support tube is mounted to the manipulator at the vessel.

Four 5 μm thick and 13 mm wide stainless-steel bands are strung at a distance of 7 mm parallel to the beam and serve as a "beam pipe".[11] Additional aluminium coating of the bands reduces the resistivity. This shielding is necessary to reduce wake fields in the vessel. Several other options for RF-shielding were studied with a half-scale model of the tank [17] with the real vessel [18] itself and with intensive simulations [19]. The bands have proven to give sufficient shielding, are mechanically robust and add a tolerable amount of material. It is foreseen to test the shielding quality of only 2 bands and thus to reduce the material by 50%.

5. Readout and slow control

The 128 input channels of a HELIX chip are multiplexed to one quasi-differential analog output and two chips are read out in daisy-chain mode. The output signals pass through 1.3 m long coaxial cables to the inner side of a ring-shaped PCB. This PCB (one for two double-sided detectors) serves as a feedthrough (secondary vacuum inside, atmosphere outside) and is sealed on the two planar surfaces with O-rings. Close to the feedthrough mounted onto the vacuum flange are differential receivers and LEDs (1A194 from ABB) for analog optical data transmission with up to 40 MHz. 576 fibers (200 μm thick) transmit the light from all superlayers to the electronics trailer where the digitization occurs on the Front End Driver (FED) boards. The data are stored in memory on the second level buffer and are eventually analyzed by a second level trigger processor.

[9] Produced by Rasant-Alcotec, Germany.

[10] Small leaks is the welding seam or in the cap itself are closed with the low out-gasing Stycast 2850 FT epoxy.

[11] During injection the distance is 20 mm.

Only six digital signals are needed to operate a HELIX. These signals originate from the FED Controller card in the trailer and are transmitted optically to a fanout which is located close to the vessel.[12] This way we avoid any ground connection between the electronics trailer and the vessel.

Since the chips and strip detectors are operated in vacuum, cooling is vital and in case of insufficient cooling, the chip power has to be turned off. There are six Pt-100 sensors in every module which are connected to a TempScan[13] unit. This device not only supports computer readout of temperatures but also features hardware alarm outputs with programmable thresholds. After configuration these alarms work independently of any further computer connection and are inputs to a Programmable Logic Control (PLC), Simatic-S5,[14] which controls the chip power supplies.

Power cuts are another concern. If the bias voltage were to drop suddenly from 400 V to zero there would be a high risk of damaging the strip detectors and bonds. Therefore our bias voltage power supply[15] has a hardware "ramp down" input connected to the PLC and is powered by a UPS. If a power failure is detected by the UPS the PLC automatically begins a controlled ramp down.

In addition, the PLC is the backbone of all other safety-related operations including an interlock for manipulator movements.

It is also worth mentioning that the valve, which separate the primary from the secondary vacuum, opens in case of a vacuum leak. This operation is also controlled by a PLC and is implemented to avoid a pressure difference between the vacua which would destroy the aluminium caps, and consequently all strip detectors.[16]

[12] Originally we used commercial optical receivers from Hirschmann (OEDH50M2). In the vicinity of the vessel the radiation level was too high for this device, i.e. spurious signals were generated. Our analog optical receivers together with discriminators work without any problem.

[13] Produced by IOtech, USA.

[14] Produced by Siemens, Germany.

[15] EHQ8000F produced by Gleisberg, Germany.

[16] The caps will deform if the pressure difference is larger than 10 mbar.

6. Installation at DESY

The first three prototype detectors were installed in 1996 at DESY and replaced in 1997. Experiences gained with these modules were reported earlier [20].

In spring 1998 a substantial number of modules was installed with a close-to-final design (fifteen double-sided and three single-sided detectors). This number was large enough for standalone track finding in a small acceptance region and was thus used to develop and test track finding and alignment software. In addition, the integration of the VDS into the HERA-B data acquisition, slow control and software environment is complete. This also includes routine operation of the Roman Pots.

Fig. 6 show S/N plots for a typical double-sided detector and for a detector with the final design (HELIX version 2.2 instead of 2.1 and an improved hybrid) installed in winter 1998. The data quality of the final design is obviously much better. With these S/N ratios, single-hit efficiencies of about 90% and 99% have been measured for the older and the final designs, respectively.

Two algorithms for standalone track finding have been developed. Even though most of the superlayers are in a magnetic field-free region the large number of strip clusters[17] poses a challenge to the algorithms. The number of ghost tracks especially has to be kept at a low level without compromising the reconstruction efficiency.

One algorithm, called HOLMES [21] uses all possible combinations of two x- and two y-view planes in neighboring superlayers to define track candidates pointing to the target. In the next step, confirmation hits in other planes are searched for, and a Kalman filter is applied to update the track parameters with every new hit. Finally, in the case where one hit is shared by several candidates, a quality parameter decides which track this hit belongs to. The hits not included in tracks pointing to the target can be used to reconstruct particles from secondary decays such as those from K_S.

[17] On average there are 600 track hits per bunch crossing with four interactions, and in addition there are noise hits.

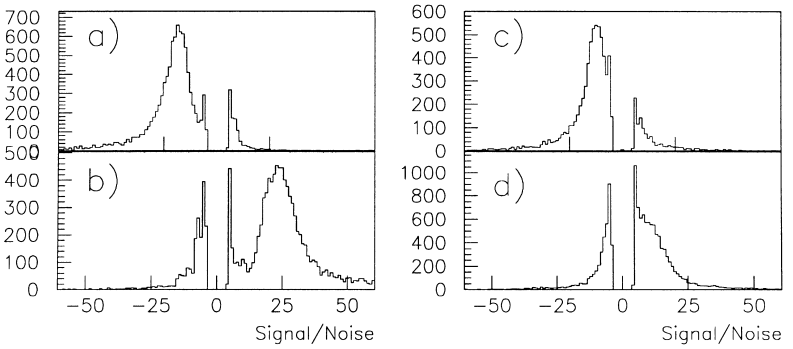

Fig. 6. S/N for two different strip detectors. (a) and (b) for p-side and n-side of the final design detector, respectively, (c) and (d) for an prototype detector from 1998.

The second algorithm, Cellular Automaton for Track Search (CATS) [22,23] first creates a list of all possible track segments pointing to the target from hits in neighboring superlayers. Optionally space points or projections are used. Starting from the downstream end two consecutive segments (one between superlayers 7 and 8 and one between 6 and 7) are merged if they share a hit (in layer 7) and if their slopes are similar. The track quality is determined by the number of incorporated segments, after the merging process has stepped through all superlayers. As for HOLMES a reduced hit list can then be used to reconstruct tracks from secondary decays.

Fig. 7 shows a performance study with MC events. The reconstruction efficiency for tracks with a momentum larger than 1 GeV/c and the rate of ghost tracks are plotted as a function of the number of interactions per bunch crossing. Both algorithms meet the specifications.

Using these tracking codes, target spots ((x, y) of tracks at z_{target}) can be reconstructed. Fig. 8 shows the reconstructed x position of the target versus time for a run with a single wire in operation. Overlayed is the position as determined from the mechanical steering of the wire. There is perfect agreement between the two measurements. Note that wire position was constantly adjusted to keep the interaction rate stable. The position along the wire can also be reconstructed with the VDS, and thus in the case where all wires are inserted the beam profile can be accurately measured. Consequently, our detector will not only be used for physics but will become a useful tool for beam diagnostics at the HERA storage ring.

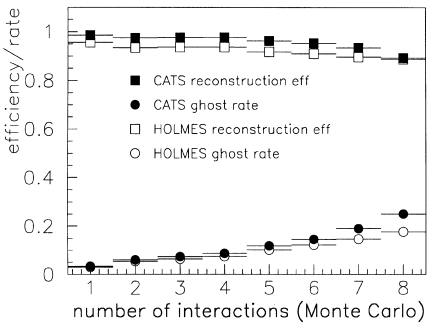

Fig. 7. Reconstruction efficiency and ghost rate for HOLMES and CATS versus the number of interactions per bunch crossing. The single-hit efficiency was 96% in this study.

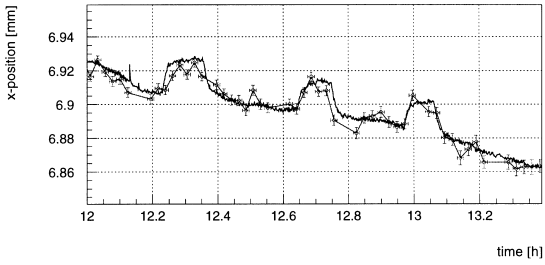

Fig. 8. VDS reconstructed target position (crosses) versus time. Overlayed is the wire position (line) measured by the mechanical steering.

7. Summary

The hardware of the silicon vertex detector is largely installed. This is true of the strip detectors themselves and of the infrastructure.

From our irradiation studies of the strip detectors and the HELIX chips we expect them both to be functional for at least one year in the high-radiation environment of HERA-B. The experience with last year's installation prove that we can operate the vertex detector. This includes the integration of the vacuum vessel into the storage ring without disturbing the proton beam, the operation of the Roman Pots, the readout chain, the slow control and the reconstruction software.

The entire detector will be completed by the end of the year.

References

[1] E. Hartouni et al., HERA-*B* Technical Design Report, DESY-PRC 95/01, January 1995.
[2] I. Abt et al., Nucl. Instr. and Meth. A 423 (1999) 303.
[3] I. Abt et al., Nucl. Instr. and Meth. A 430 (2000) 112.
[4] S. Amato et al., LHC*b* Technical Proposal, CERN/LHCC 98-4, LHCC/P4, 20 February 1998.
[5] M. Eberle, Untersuchung eines typeinvertierten Silizium-Streifenzählers mit der Aulesekette des HERA-B Vertexdetektors des Jahres 1996, Diploma Thesis, May 1997, University of Heidelberg.
[6] P. Azzi et al., Nucl. Instr. and Meth. A 383 (1996) 155.
[7] ATLAS Inner Detector Technical Design Report CERN/LHCC/97-17.
[8] L. Andricek et al., Nucl. Instr. and Meth. A 409 (1998) 184.
[9] K. Riechmann, K.T. Knöpfle, V.M. Pugatch, Nucl. Instr. and Meth. A 377 (1996) 276.
[10] V.M. Pugatch et al., Radiation hardness of the HERA-B strip detectors, Fourth International Conference on Large Scale Applications and Radiation Hardness of Semiconductor Detectors, June 1999, Florence, submitted for publication in Nuovo Cimento.
[11] M. Feuerstack-Raible, Nucl. Instr. and Meth. A 447 (2000) 35, these proceedings.
[12] S. Brenner et al. (RD20 Collaboration), Nucl. Instr. and Meth. A 339 (1994) 564.
[13] W. Fallot-Burghardt, A CMOS mixed-signal readout chip for the microstrip detectors of HERA-B, Ph.D. Thesis, June 1998, University of Heidelberg.
[14] U. Trunk, Radiation tolerance of the HELIX128-2.2 chip for the HERA-B experiment, Ph.D. thesis, July 2000, University of Heidelberg.
[15] W. Fallot-Burghardt et al., HELIX128S-2 Users Manual, HD-ASIC-33-0697, http://wwwasic.ihep.uni-heidelberg.de/feuersta/projects/Helix/index.html.
[16] I. Abt et al., Nucl. Instr. and Meth. A 411 (1998) 191.
[17] F. Galluccio et al., Measurement of the longitudinal coupling impedances of the HERA-B vertex detector chamber, DESY-M-96-13G.
[18] F. Klefenz et al., First results from measurements of modes in the HERA-B vertex chamber excited by the proton beam, DESY-M-97-01.
[19] F. Klefenz, Die Hochfrequenz-Abschirmung des HERA-B Vertexdetektors, Diploma Thesis, June 1997, University of Heidelberg.
[20] C. Bauer et al., Nucl. Instr. and Meth. A 418 (1998) 65.
[21] M. Schmelling, The HOLMES Program Package, HERA-B Internal Note 99-086.
[22] I. Kisel, Nucl. Instr. and Meth. A 387 (1997) 443.
[23] I. Kisel, S. Masciocchi, CATS: a cellular automaton for tracking in silicon for the HERA-B vertex detector, HERA-B Internal Note 99–242.